



Technical note: *in situ* measurement of flux and isotopic composition of CO₂ released during oxidative weathering of sedimentary rocks

Guillaume Soulet¹, Robert G. Hilton¹, Mark H. Garnett², Mathieu Dellinger¹, Thomas Croissant¹, Mateja Ogrič¹ and Sébastien Klotz³

5 ¹Department of Geography, Durham University, South Road, Durham DH1 3LE, United Kingdom

²NERC Radiocarbon Facility, Rankine Avenue, East Kilbride, Glasgow G75 0QF, UK

³IRSTEA Grenoble, 2 rue de la papeterie, BP 76, 38402 Saint-Martin-d'Hères, Cedex, France

Correspondence to: Guillaume Soulet (guillaume.s.soulet@durham.ac.uk)

Abstract. Oxidative weathering of sedimentary rocks can release carbon dioxide (CO₂) to the atmosphere and is an important natural CO₂ emission. Two mechanisms operate – the oxidation of sedimentary organic matter and the dissolution of carbonate minerals by sulphuric acid. It has proved difficult to directly measure the rates of these weathering processes in the field, with previous work generally using indirect methods which track the dissolved products of these reactions in rivers. Here we design a chamber method to measure CO₂ production during the oxidative weathering of shale bedrock, which can be applied in erosive environments where rocks are exposed frequently to the atmosphere. The chamber is drilled directly into the rock face and is a relatively low cost method to provide a long-lived (several months or more), oxygenated environment in contact with a surface area of potential reactant. To partition the measured CO₂ fluxes and the source of CO₂, we use zeolite molecular sieves to trap CO₂ ‘actively’ (over several hours) or ‘passively’ (over a period of months). The approaches produce comparable results, with the trapped CO₂ having a fraction modern ranging from 0.05 to 0.06 and demonstrating relatively little contamination from local atmospheric CO₂ (fraction modern of 1.01). We use stable isotopes of the trapped CO₂ to partition between an organic and inorganic carbon source. The measured fluxes of rock-derived organic matter oxidation and carbonate dissolution by sulphuric acid from a single chamber were high, but consistent with the high erosion rate of the study region (of ~5 mm yr⁻¹). We propose our *in situ* method has the potential to be more widely deployed to directly measure CO₂ fluxes during the oxidative weathering of sedimentary rocks, allowing for the spatial and temporal variability in these fluxes to be determined.

25 1 Introduction

The stock of carbon contained within sedimentary rocks is vast, with ~1.25×10⁷ PgC contained within organic matter and ~6.53×10⁷ PgC as carbonate minerals (Sundquist and Visser, 2005). If these rocks are exposed to Earth’s oxygenated surface, for instance during rock uplift, erosion and exhumation, oxidative weathering can result in a release of carbon dioxide (CO₂) from the lithosphere to the atmosphere (Petsch et al., 2000). There are two main processes to consider: i) the oxidation of rock-



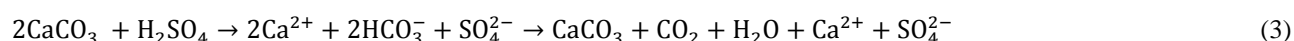
derived organic carbon (Berner and Canfield, 1989; Petsch, 2014), which can be expressed by the (geo)respiration of organic matter:



and ii) the oxidation of sulphide minerals (e.g., pyrite) which produces sulphuric acid, which can chemically weather carbonate minerals and release CO_2 (Calmels et al., 2007; Li et al., 2008; Torres et al., 2014) by the reaction:



or



In the case of Eq. (1) and Eq. (2), CO_2 is released to the atmosphere “immediately”. In the case of Eq. (3), CO_2 is released to the atmosphere over a timescale equivalent to that of the precipitation of carbonate in the ocean ($\sim 10^4$ to 10^6 years; Berner and Berner, 2012).

The fluxes of carbon transferred to the atmosphere in response to both oxidative weathering processes are thought to be as large as that released by volcanic degassing, but the absolute fluxes remain uncertain (Li et al., 2008; Petsch, 2014). As such, both processes act to govern the levels of atmospheric CO_2 and O_2 , and hence Earth’s climate over geological timescales (Berner and Canfield, 1989; Torres et al., 2014). The oxidation of rock-derived organic carbon may also contribute to modern biological cycles, especially rock substrate that is rich in organic carbon (Bardgett et al., 2007; Copard et al., 2007; Keller and Bacon, 1998; Petsch et al., 2001). Various approaches have been adopted to better quantify these major geological CO_2 sources. These include the use of geochemical proxies in rivers, which indirectly track the oxidative weathering of sedimentary rocks at the catchment-scale. For instance, the trace element rhenium has been used to compare relative rates of rock-derived organic carbon oxidation (Jaffe et al., 2002) and estimate the corresponding fluxes of CO_2 across river catchments (Dalai et al., 2002; Hilton et al., 2014; Horan et al., 2017). Another approach has been to measure the loss of radiocarbon-depleted organic matter in river sediments during their transfer across the floodplains of large river basins (Bouchez et al., 2010; Galy et al., 2008). In the case of sulphuric acid-weathering of carbonate minerals, the dissolved sulphate flux can be informative if the source of SO_4^{2-} has been assessed using sulphur and oxygen isotopes (Calmels et al., 2007) and/or using the dissolved inorganic carbon flux and its $\delta^{13}\text{C}$ composition (Galy and France-Lanord, 1999; Li et al., 2008).

It should be possible to directly measure the flux of CO_2 emanating from sedimentary rocks in response to oxidative weathering. Keller and Bacon (1998) explored such an approach in a 7 m deep soil on till, suggesting geo-respiration of Cretaceous age organic matter was an important source of CO_2 at depth. However, this research has not to our knowledge been replicated, nor applied in erosive landscapes where sedimentary rocks are frequently exposed to weathering by erosion



processes (Blair et al., 2003; Hilton et al., 2011). In these locations, oxidative weathering fluxes are thought to be very high (Calmels et al., 2007; Hilton et al., 2014; Petsch et al., 2000). One of the challenges of tracking CO₂ directly is that flux measurements must be combined with the isotopic composition (¹²C, ¹³C and ¹⁴C) of the CO₂ (Keller and Bacon, 1998). Only with that information can the measured CO₂ flux be partitioned into the component derived from the oxidation of rock-derived carbon and that derived from the dissolution of carbonate (in addition to inputs from the modern plant and soil biosphere, and atmospheric inputs).

The objective of this paper is to provide a detailed proof of concept study of methods we have designed which can: (1) make direct measurements of the flux of CO₂ released during the oxidative weathering of sedimentary rocks; and (2) trap the CO₂ produced during weathering in order to measure its isotope composition, and partition the source of the CO₂ flux between rock-derived organic carbon and carbonate. Here we outline the chamber-based method to measure CO₂ fluxes, and provide the first examples of active and passive methods to trap CO₂ and use its isotope composition to directly quantify the rate of weathering reactions.

2 Method

2.1 Study area

The study location is within the Laval catchment, part of the IRSTEA Draix Bléone Experimental Observatory and the Réseau des Bassins Versants network, located near the town of Draix, Alpes de Haute Provence, France. The small catchment (0.86 km²) is heavily instrumented, with continuous monitoring of rainfall, river water discharge, river solid load transport, total dissolved fluxes and physical erosion rates over the last four decades (Cras et al., 2007; Mathys et al., 2003). These measurements provide hydrodynamic and geomorphic context for any studies of oxidative weathering. The lithology of the catchment is composed of Callovo-Oxfordian marls, which contain inorganic carbon and organic matter (Graz et al., 2012). Sulphide minerals are widespread as disseminated pyrite and veins which outcrop in the catchment (Cras et al., 2007). The rock-strength, climate and geomorphic setting combine to produce a badland-type morphology with very steep and dissected slopes. Erosion rates are very high, with sediment export fluxes of 11,200 tons.km⁻².yr⁻¹ on average during the period 1985 to 2005 AD (with a minimum of 4,400 tons.km⁻².yr⁻¹ in 1989 and a maximum of 21,100 tons.km⁻².yr⁻¹ in 1992) (Graz et al., 2012; Mathys et al., 2003). Assuming an average rock density of ~2.2 t m⁻³, this equates to a physical erosion rate of ~5 mm yr⁻¹. These features limit the development of soils, typically 20-to-30-cm thick where they are present at all. As a result, it is easy to find regolith and rock surfaces that are devoid of soils and roots, and where sedimentary rocks are directly exposed to the oxygen-rich atmosphere.

2.2 Natural oxidation and CO₂ accumulation chambers

In order to measure the flux of CO₂ produced by oxidative weathering of sedimentary rocks, and accumulate enough CO₂ to perform carbon isotope measurements, we use accumulation chambers (e.g., Billett et al., 2006; Hardie et al., 2005). These



have been extensively used to measure soil respiration (e.g., Hahn et al., 2006; Hardie et al., 2005), CO₂ evasion by streams and rivers (e.g., Billett et al., 2006; Borges et al., 2004), but have not yet been used to examine rock-atmosphere interactions. Because most fine-grained sedimentary rocks have a degree of competency, accumulation chambers can be made by directly drilling into the rock. Here we use a rock-drill to make 40 cm-long chambers with an inner diameter of 29 mm. Our aim was to minimise the volume of the chamber while maximizing the surface of exchange with the surrounding rock.

After measuring the dimensions of the chamber, its entrance is fitted with a small PVC tube (~3cm-diameter, ~3cm-long), which allows a tight seal with an inserted rubber stopper containing two holes. Two Pyrex® tubes (ID=3.4mm and OD=5mm; one of 12cm-long and one of 7cm-long) are inserted through the rubber stopper. The differential length is to improve airflow in the chamber while in operation. The sections of the Pyrex® tubes sticking out of the chamber are fitted with Tygon® tubing (E-3603; Saint Gobin, France). To isolate the accumulation chamber from the atmosphere as best as possible, the Tygon® tubing is sealed with WeLock® clips (Scandinavia Direct Ltd, UK) and silicone sealant (Unibond® Outdoor) is placed around the entrance of the chamber (the 3cm-diameter PVC tubing and the rubber stopper) (Figure 1). The newly installed chamber is left for ~2 days to allow the sealant to fully dry. Here we acknowledge that a perfect seal is impossible, due to the natural rock fracturing around the chamber. Table 1 summarises the dimensions of an example chamber drilled and sealed in the field on 13th December 2016.

Drilling results in the formation of an oxidative weathering zone by introducing an oxygen-rich atmosphere in the chamber. If gaseous O₂ is consumed (e.g. by Eq. (1)), this would create a gradient in the partial pressure of O₂ (pO₂) whereby the atmosphere surrounding the rock and chamber is of higher pO₂. Given the natural porosity and permeability of the shale bedrock, any diffusion of O₂ is likely to be into the chamber. This should act continuously to fuel the chamber with oxygen. In contrast, if CO₂ is produced inside the chamber (by Eq. (1) and Eq. (2)) then the partial pressure of CO₂ (pCO₂) will exceed that of the atmosphere. The result is that for chambers where oxidative weathering is occurring, the ingress of and ‘contamination’ by atmospheric CO₂ should be minimal, and there should be a supply of O₂ for reactions. These inferences can be tested using a pO₂ probe and by trapping CO₂ and measuring its isotope composition.

In this example we aimed to measure oxidation of sedimentary rocks, and intended to minimise the role of CO₂ produced by root respiration. Therefore, the chambers were drilled on cleared rock surface, devoid of visible roots. The rock powder produced when drilling the chambers was collected, freeze-dried and grinded to fine powder for measurement of its organic-inorganic carbon content and its isotopic composition.

2.3 CO₂ flux measurements

A closed-loop CO₂ sampling system similar to the molecular sieve sampling system (MS³) described in Hardie et al. (2005) was used for CO₂ flux measurements and CO₂ sampling (Figure 1). The system incorporated the following components: an air filter, a water trap (cartridge filled with magnesium perchlorate), a portable infrared gas analyser (IRGA) equipped with an internal air pump, calibrated to a pCO₂ range of 0 to 5000 ppmv and installed with an pO₂ probe (EGM-5, PP Systems, UK), a CO₂ scrub (cartridge filled with soda lime), a bypass, and a set of WeLock® clips that allows the air flow to be diverted



through the bypass or the CO₂ scrubber cartridge. Optionally a zeolite molecular sieve sampling cartridge can be inserted in the line (see next section).

Before each CO₂ flux measurement, the Tygon® tubes exiting the chamber were fitted with autoshutoff Quick Couplings™ (Colder Products Company, USA), and the CO₂ contained within the sampling system is removed using the CO₂ scrubber cartridge. When no CO₂ is left in the sampling system (as indicated by the IRGA), the air flow is diverted through the bypass, and the system connected to the chamber (Figure 2). The use of the auto-shutoff couplings prevents atmospheric contamination at the moment of connection to the chamber. Then, pCO₂ in the chamber is lowered to near atmospheric pCO₂ by guiding the air flow through the CO₂ scrubber cartridge. We let the CO₂ accumulate in the chamber for several minutes (typically 10 minutes) by guiding the air flow through the bypass (Figure 2). This operation can be repeated several times to provide multiple measurements of CO₂ flux over a period of hours (Figure 3). The CO₂ evolution in the chamber typically shows a curvature, the curve flattening with time and higher concentration (Figure 3). In order to calculate the CO₂ flux, we first convert the pCO₂ measurements into the mass of carbon contained in the chamber:

$$m = \frac{p\text{CO}_2}{10^6} \cdot V \cdot A \quad (4)$$

where m is the mass of carbon in the chamber (in mgC), $p\text{CO}_2$ the concentration of CO₂ in the chamber in ppm (cm³.m⁻³), V is the total volume (cm³) i.e., the sum of the volume of the chamber (V_{CH}) and the volume of the CO₂ sampling system (V_L) when air flows through the bypass. Factor A converts centimetres cubed of CO₂ into milligrams of carbon, depending on temperature and pressure following the ideal gas law:

$$A = \frac{P \cdot M_C}{R \cdot T} \cdot 10^{-3} \quad (5)$$

where P is the pressure (Pa) as measured by the IRGA, M_C is the molar mass of carbon (g.mol⁻¹), R is the gas constant (m³.Pa.K⁻¹.mol⁻¹) and T the temperature (K) in the chamber. Then the rate (q in mgC.min⁻¹) at which carbon accumulates in the chamber is calculated using an exponential model (described below; Pirk et al., 2016) and converted into a flux of carbon (Q in gC.m².yr⁻¹) emitted to the atmosphere under the form of CO₂ using:

$$Q = \frac{q}{S} \cdot 525.6 \quad (6)$$

where, 525.6 converts mgC.min⁻¹ into gC.yr⁻¹, and S (m²) is the inner surface area of the chamber exchanging with the surrounding rock. To calculate the rate of accumulation of carbon (q) in the chamber we use the exponential model described by Pirk et al. (2016):

$$\frac{dm(t)}{dt} = q - \lambda(m(t) - m_0) \quad (7)$$



where $\frac{dm(t)}{dt}$ is the carbon mass change in the chamber with time. Parameter m_0 is the mass of carbon in the chamber at the beginning of the CO₂ accumulation and that should be close to the mass of carbon in the chamber at atmospheric pCO₂. The constant λ (in units of time⁻¹, here in min⁻¹) describes the sum of all processes which are proportional to the carbon mass difference $\Delta m(t) = m(t) - m_0$ and responsible for the curvature of the carbon mass accumulation evolution (Figure 3). The model does not a priori assume any process to be responsible for the curvature (Pirk et al., 2016). In the case of the measurement of CO₂ flux in soils, the curvature (λ) relates to leakages, diffusivity from soil CO₂ into the chamber headspace and photosynthesis (Kutzbach et al., 2007). In the case of our chambers drilled in rock, since it is assumed that there is no possibility of photosynthesis, λ likely relates to the diffusivity of carbon from the rock to the chamber headspace and to the chamber leakiness. Equation Eq. (7) is solved by fitting the following function to the data (Figure 3B):

$$m(t) = \frac{q}{\lambda} (1 - \exp(-\lambda t)) + m_0 \quad (8)$$

For the sake of comparability and automatization, all curves of carbon mass accumulation were fitted for periods of 6 minutes after the rate of carbon mass change variability over a moving 10-second window was below a certain threshold (1×10^{-4} mg.s⁻¹ for 20 seconds was empirically found suitable; Figure 3B).

Several parameters lead to uncertainties on the flux calculations. They are all related to the conversion of pCO₂ to mass of carbon (Table 1): i) the volume of the chamber (V_{CH}); ii) the surface area of exchange with the surrounding rock (S); iii) the volume of the closed-loop system when air flows through the bypass (V_L was determined to be 127.8 ± 0.5 cm³ through an experiment of successive CO₂ dilution in a known volume); and iv) the temperature in the chamber was assumed to range from 0 to 20°C over the course of the experiment. We estimated the relative uncertainty on the measured flux using a Monte-Carlo simulation of error propagation using the ranges listed above and in Table 1. The resulting relative uncertainty on the measured flux was estimated to be within ± 2.5 %. An additional relative uncertainty linked to the rate of CO₂ accumulation in the chamber (parameter q obtained through fitting the exponential model to the data) ranges between 0.5 to 1.0%. Altogether, the final relative uncertainty determined with our Monte-Carlo simulation of error propagation was found to be within ± 2.7 %. In the case that the relative standard deviation on multiple flux measurements is higher than 2.7%, we adopt the standard deviation as the uncertainty.

2.4 CO₂ sampling and isotopic analysis

CO₂ evading the rock accumulates in the chamber and can be sampled using a zeolite molecular sieve trap (Garnett et al., 2009; Garnett and Hardie, 2009; Hardie et al., 2005). Zeolites have a high affinity for polar molecules such as H₂O and CO₂, and are widely used to separate CO₂ from air at ambient temperature and pressure. The gas trapped by the zeolite sieve can be extracted in the laboratory at high temperature for CO₂ purification and isotope analysis (Garnett and Murray, 2013; Hardie et al., 2005). The type of zeolite (13X) and the design of the cartridge containing the zeolite, is described by Hardie et al. (2005) and Garnett et al. (2009). In our study the CO₂ was sampled ‘actively’ – i.e., using the CO₂ sampling system coupled to the



pump incorporated in the IRGA to force the air through the zeolite molecular sieve cartridge (Figure 1) following Hardie et al. (2005). Two approaches can be used. The first involves connection of the line to the chamber for the duration of trapping, which was used on 27/03/2017. Each removal of CO₂ onto the trap can be controlled to return the chamber to ambient atmospheric pCO₂, allowing for a subsequent measurement of CO₂ flux (Figure 3). The second approach allows pCO₂ to accumulate in the chamber, before attaching the scrubbed line and removing the CO₂, which we tested on 30/03/2017. The benefit of the latter method is that it allows the gas line and IRGA to be used for other tasks while in the field, but may be more susceptible to atmospheric inputs during the connection of lines.

The CO₂ was also sampled ‘passively’, when the zeolite molecular sieve is connected to the chamber for several months following the procedure described in Garnett et al. (2009) (Figure 4). This approach has the benefit of providing an integrative view of CO₂ production over longer periods of time. A passive trap was installed on the 15th December 2017 (2 days after the chamber was constructed) and removed on the 26th March 2017 (101 days after its installation) for chamber H6. Based on previous work (Garnett et al., 2009; Garnett and Hardie, 2009), it is expected that the passive trap method can lead to an isotope fractionation of $\delta^{13}\text{C} \sim 3.50 \pm 0.45 \text{ ‰}$ associated with the diffusion of CO₂ from the chamber to the zeolite trap. In addition, a sample of local atmospheric CO₂ was also collected by actively circulating the atmosphere sampled at $\sim 3\text{m}$ elevation above the valley floor through a zeolite molecular sieve.

After sample collection the zeolite molecular sieves were sealed with WeLock® clips on either end before being disconnected from the sampling system (active or passive) and returned to the NERC Radiocarbon Facility for CO₂ recovery. The CO₂ collected was desorbed from the zeolite by heating (425°C) and cryogenically purified (Garnett and Murray, 2013). One aliquot of the recovered CO₂ was used for $\delta^{13}\text{C}$ measurement using Isotope Ratio Mass Spectrometry (IRMS; Thermo Fisher Delta V; results expressed relative to the VPDB standard). A further aliquot was converted to graphite and analysed for ¹⁴C using accelerator mass spectrometry at the Scottish Universities Environmental Research Centre. Radiocarbon results were, following convention, corrected for isotopic fractionation using the measured sample IRMS $\delta^{13}\text{C}$ values, and reported in the form of the fraction modern (Fm) [Stuiver and Polach (1977); corresponding to ¹⁴a_N in Mook and van der Plicht (1999), or F¹⁴C in Reimer et al. (2004)] (Table 2).

2.5 Partitioning the sources of CO₂

As the chamber was drilled away from the obvious influence of root respiration, the CO₂ emanating from the rock should originate from: i) the oxidation of the organic carbon contained within the rock mass following Eq. (1); and/or from ii) the dissolution of the carbonate minerals by sulphuric acid following Eq. (2). Some of the CO₂ collected in active or passive zeolite molecular sieves might also originate from atmospheric CO₂ (see discussion below). To correct for possible atmospheric contamination, and partition the sources of CO₂, we solve the following isotope-mass balance system:



$$\begin{cases} f_{\text{Atm}} + f_{\text{Rock OC}} + f_{\text{Carb}} = 1 \\ f_{\text{Atm}} \cdot \delta^{13}\text{C}_{\text{Atm}} + f_{\text{Rock OC}} \cdot \delta^{13}\text{C}_{\text{Rock OC}} + f_{\text{Carb}} \cdot \delta^{13}\text{C}_{\text{Carb}} = \delta^{13}\text{C}_{\text{Chamber}} \\ f_{\text{Atm}} \cdot \text{Fm}_{\text{Atm}} + f_{\text{Rock OC}} \cdot \text{Fm}_{\text{Rock OC}} + f_{\text{Carb}} \cdot \text{Fm}_{\text{Carb}} = \text{Fm}_{\text{Chamber}} \end{cases} \quad (9)$$

where, f_{Atm} is the mass fraction of CO_2 originating from the atmosphere, $f_{\text{Rock OC}}$ is that originating from the oxidation of the rock-derived organic carbon and, f_{Carb} is that originating from carbonate dissolution by sulphuric acid. Subscript ‘‘Chamber’’ stands for CO_2 sampled from the chambers and extracted from the zeolite molecular sieves.

5 The $\delta^{13}\text{C}$ composition (vs. VPDB) of the rock-derived organic carbon was obtained by IRMS after inorganic carbon removal from the rock powdered samples by HCl fumigation, followed by closed-tube combustion to produce CO_2 . The $\delta^{13}\text{C}$ composition of the carbonates was obtained after dissolution of the carbonates of the rock powdered samples by phosphoric acid in vacuumed vessels following standard procedures at NERC Radiocarbon Facility (East Kilbride, UK). Since the rock-derived organic carbon and carbonates were formed millions of years ago they should contain radiocarbon levels close to the
10 AMS background (Table 3).

3 Results and Discussion

Here we present the results obtained from a natural weathering chamber (H6) drilled in December 2016. Our aim is to assess the feasibility of the method, in terms of: i) measuring the fluxes of CO_2 ; ii) collecting sufficient mass of CO_2 for isotope analysis (to partition between organic and inorganic derived CO_2); and iii) checking the role of atmospheric CO_2 contamination
15 for both the active and passive CO_2 sampling methods. We discuss the results from chamber H6 in the context of using this method more widely to better quantify rates of oxidative weathering and associated CO_2 release.

3.1 Flux Measurements

Three months after the installation of the chamber H6, CO_2 fluxes were measured alongside a series of zeolite-trapping events on 27/03/2017 (Figure 3). If the chamber was perfectly isolated from the atmosphere, then we might expect the rate of carbon
20 accumulation ($\frac{dm(t)}{dt}$) to be constant, while it decreases with time. As expected, this indicates that the chamber is not perfectly sealed. This has some important implications. First, the leak rate depends on the $p\text{CO}_2$ gradient between the chamber and the atmosphere. Since this gradient is positive in the chamber (Figure 2) ($p\text{CO}_{2\text{chamber}} > p\text{CO}_{2\text{atmosphere}}$), then CO_2 likely diffuses from the chamber to the atmosphere. This has the advantage that it naturally minimizes any atmospheric CO_2 contamination. Conversely, since the CO_2 production is linked to the consumption of O_2 , then the O_2 gradient is expected to
25 be negative ($p\text{O}_{2\text{chamber}} < p\text{O}_{2\text{atmosphere}}$), and thus atmospheric O_2 naturally diffuses inside the chamber. This means that the chamber can be closed for months and still contain gaseous O_2 . Our measurements of O_2 using the EGM-5 O_2 probe suggest that the chamber had a similar $p\text{O}_2$ as that contained in the ambient atmosphere of the catchment (the chamber value was 96 to 99% of the atmosphere $p\text{O}_2$).



The fluxes of CO₂ measured in this chamber on 27/03/2017 decreased from 529 ± 14 gC.m⁻².yr⁻¹ to 266 ± 7 gC.m⁻².yr⁻¹ with the number of times we extracted the CO₂ from the chamber (Figure 3). The flux becomes approximately constant after three CO₂ extractions during zeolite trapping, with an average of 272 ± 8 gC.m⁻².yr⁻¹ (1sd, n=4) for the last 4 repeats (Figure 3). This observation might be explained by the fact that over time (days to months), CO₂ accumulates not only in the chamber, but also in the rock pores surrounding the chamber. Weathering reactions are likely to occur not only at the chamber-rock interface, but also into the rock mass over several centimetres. When CO₂ is first extracted from the chamber, the CO₂ stored in the surrounding pores quickly refills the chamber. It appears that after three extractions this CO₂ is depleted, meaning that the more constant values correspond to the actual flux of CO₂ through the surface area of the chamber. We would therefore recommend that flux measurements are made on such a chamber following ~3 to 4 removals of CO₂. It remains to be seen the degree to which this feature is widespread, or chamber specific.

3.2 Isotope measurements

The atmospheric CO₂ was sampled on 27/03/2017, yielding a δ¹³C of -9.6‰ and a ¹⁴C activity of Fm=1.0065±0.0044. From chamber H6, we sampled CO₂ twice actively on 27/03/2017 (by in line trapping, Figure 3) and on 29/03/2017 (by repeated trapping over the course of a day) both yielding ~2.1 mgC. The ¹⁴C activities (Fm of 0.0597±0.0047 and 0.0562±0.0047, respectively) were identical within measurement uncertainty. Because the CO₂ originating from rock-derived organic matter and carbonate minerals is ‘¹⁴C-dead’, as confirmed by ¹⁴C measurements of the organic carbon and carbonate of the rock from the studied chamber (Table 3), the atmospheric CO₂ input can be calculated as $100 \times \frac{Fm_{\text{Chamber}}}{Fm_{\text{Atm}}}$ %. The Fm from both samples show that only ~5.5% to 6% of the CO₂ trapped was of atmospheric origin and that the two active trapping methods produce comparable results. The δ¹³C compositions (-7.4‰ and -6.1‰, respectively) were within the range expected for a mixture of organic and inorganic carbon derived CO₂, but differed by ~1 ‰ for these two traps. The difference may reflect different relative rates of sulphide versus organic matter oxidation over a daily timescale, which is an observation worth exploring in more detail.

From chamber H6, the CO₂ sample passively trapped for 101 days from mid-December 2016 to late March 2017 yielded ~11.4 mgC. The sieve cartridges have been shown to reliably trap >100 ml CO₂ (Garnett et al., 2009; i.e. > ~50 mgC), so the 11.4 mgC from H6 represents less than a quarter of the sieve capacity, suggesting that passive sieves can be left for at least ~6 months without becoming saturated with CO₂ (in reality, saturation by water vapour may be more likely to be a limiting factor). The Fm was 0.0495±0.0047, which is very similar to the active trapping results, with only ~5% atmospheric CO₂. This is perhaps surprising since the trap was left exposed in the natural environment for three months. However, it results from the high pCO₂ present in the chamber throughout the time period, driving a net diffusive transfer of CO₂ from chamber to the zeolite sieve. It suggests the components used to make the chamber and its linkages are not susceptible to major leaks.

The δ¹³C composition of the passively trapped CO₂ was -9.4‰, displaying a 2.0‰ and 3.3‰ depletion when compared to the δ¹³C values obtained with the active trapping method. This suggests that fractionation during passive trapping occurred, in



agreement with Garnett et al. (2009) and Garnett and Hardie (2009) who show a $3.50 \pm 0.45\%$ fractionation associated with the passive trapping method. The fractionation is likely due to the diffusion of CO_2 through air (Davidson, 1995).

We solve the isotope-mass balance Eq. (9) for the actively trapped CO_2 from 27/03/2017 and 30/03/2017, and for the passively trapped CO_2 sample (Table 4). The $\delta^{13}\text{C}$ of the passively trapped CO_2 was corrected using the published $3.50 \pm 0.45\%$ fractionation factor (Garnett et al., 2009; Garnett and Hardie, 2009), and the ^{14}C activity of both the rock-derived organic carbon and carbonate end-member were set to 0, as their measured F_m were close to background (Table 3). We found very similar results for the three trapped CO_2 samples, yielding 5% to 6% of CO_2 from atmospheric contamination, 71% to 77% of CO_2 from the dissolution of the carbonates by sulphuric acid and 19% to 23% of CO_2 from the oxidation of rock-derived organic matter (details in Table 4).

A correction for the ingress of atmospheric CO_2 is applied to partition the measured flux of CO_2 . This shows 19% to 24% from rock-derived organic carbon and 76% to 81% from carbonate dissolution (Table 4). Therefore, for chamber H6 on 27/03/2017 for which we simultaneously measured the bulk CO_2 flux ($272 \pm 8 \text{ gC}\cdot\text{m}^{-2}\cdot\text{yr}^{-1}$), these proportions equate to a flux of $66 \pm 2 \text{ gC}\cdot\text{m}^{-2}\cdot\text{yr}^{-1}$ derived from the natural oxidation of rock organic matter, and a flux of $206 \pm 6 \text{ gC}\cdot\text{m}^{-2}\cdot\text{yr}^{-1}$ derived from the dissolution of carbonates by sulphuric acid (Table 4).

At the scale of chamber H6, these flux measurements imply that over a year 116 grams of rock would be weathered by sulphuric acid to produce the carbonate-derived CO_2 flux (i.e., 7.6 gC produced in one year from a rock with 6.52 w% of inorganic carbon). In contrast, 2210 grams of sedimentary rock would need to have been oxidized to produce the rock-organic carbon CO_2 flux (i.e., 2.4 gC produced in one year from a rock with 0.11 w% of organic carbon). The dissolution of carbonate depends on the oxidation of sulphides, and may therefore only occur locally where sulphides are concentrated. The oxidation of organic carbon appears to occur more homogeneously in the rock mass.

3.3 Natural flux of CO_2 evading sedimentary rocks

3.3.1 Rock-derived organic carbon oxidation

The flux of CO_2 originating from the oxidation of rock-derived organic carbon is difficult to assess. To our knowledge, there has only been one direct estimate of $0.5 \text{ gC}\cdot\text{m}^{-2}\cdot\text{yr}^{-1}$ using modelling of vadose CO_2 and its isotopes in Saskatchewan (Canada) (Keller and Bacon, 1998). This is 130 times lower than our estimate in the chamber H6 of the Laval catchment. This might be explained by the much lower erosion rates of the Canadian site, with deep soils and stable geomorphology, compared to the Laval catchment where erosion continuously exposes rocks to oxidative weathering (Graz et al., 2012).

CO_2 fluxes derived from the oxidation rock organic carbon have been indirectly estimated using geochemical proxies, such as dissolved rhenium fluxes in rivers (Dalai et al., 2002; Hilton et al., 2014; Horan et al., 2017). Our direct measurements obtained from a single chamber (H6) ($66 \pm 2 \text{ gC}\cdot\text{m}^{-2}\cdot\text{yr}^{-1}$) are of the same order of magnitude as that calculated in highly erosive Taiwanese catchments (5 to $35 \text{ gC}\cdot\text{m}^{-2}\cdot\text{yr}^{-1}$) (Hilton et al., 2014). It is clearly too early to directly relate these fluxes. It is likely that individual chambers have different CO_2 fluxes (possibly depending on rock heterogeneity, temperature, water supply),



and that CO₂ fluxes from a single chamber may vary throughout the year. Nevertheless, our proof of concept study suggests that direct measurements are consistent with proxy-based methods. The spatial variability in oxidation rates and its variability throughout the year are important questions which can be tested with the chamber method we describe here.

3.3.2 Carbonate dissolution by sulphuric acid

5 Inorganic carbon was the main source of the CO₂ flux measured during our experiment ($206 \pm 6 \text{ gC.m}^{-2}.\text{yr}^{-1}$). The dissolution of carbonate minerals by sulphuric acid (i.e., by oxidized sulphide minerals) is the simplest explanation (Calmels et al., 2007). An implication of this result is that in the Laval catchment, carbonates are weathered preferentially according to Eq. (2), i.e., immediately releasing CO₂ to the atmosphere. A study reporting the average anion concentrations in the Laval stream in 2002 (Cras et al., 2007) gives a low bicarbonate-to-sulphate ratio ($\frac{\text{HCO}_3^-}{\text{SO}_4^{2-}} \sim 0.35$). At first order (i.e., assuming that sulphate is
10 exclusively derived from oxidized sulphides), this observation supports the fact that carbonate weathering preferentially produces gaseous CO₂ (Eq. (2), i.e., $\frac{\text{HCO}_3^-}{\text{SO}_4^{2-}} = 0$) instead of dissolved inorganic carbon (Eq. (3), i.e., $\frac{\text{HCO}_3^-}{\text{SO}_4^{2-}} = 2$) at the weathering site. Because carbonate minerals are highly reactive, this means that the sulphuric acid weathering of carbonate minerals could produce a local CO₂ flux which starts to approach the rates of respiration in modern soils (e.g., Pirk et al. 2016).

The published river ion data can be used to estimate the weathering of carbonate minerals by sulphuric acid. From the average
15 Ca²⁺ and SO₄²⁻ concentrations measured in 2002 and the average runoff (Cras et al., 2007), assuming that the weathering of carbonates produced only gaseous CO₂, we estimate a flux of CO₂ to the atmosphere of 19 to 37 gC.m⁻².yr⁻¹. These values could be refined by measurement of sulphur and oxygen isotopes of SO₄²⁻ to partition sulphate source (Calmels et al., 2007). Although of the same order of magnitude, the river ion flux estimate is much lower than our direct measurement. This is likely due to the fact that we compare here an isolated (metre-scale) measurement to a catchment-scale average estimate which takes
20 into account regions that have lower erosion and weathering rates.

Our local direct measurement is higher than the flux obtained for a similar highly erosive catchment in Taiwan (Liwu River) using dissolved river chemistry and showing a value of $\sim 20 \text{ gC.m}^{-2}.\text{yr}^{-1}$ (Calmels et al., 2011; Das et al., 2012; Torres et al., 2014). These values are much higher than that of less erosive major river systems like the Mackenzie River in Canada (Calmels et al., 2007; Torres et al., 2014) ($< 1 \text{ gC.m}^{-2}.\text{yr}^{-1}$) or the Ganges-Brahmaputra river system in India ($< 1 \text{ gC.m}^{-2}.\text{yr}^{-1}$) (Galy and
25 France-Lanord, 1999; Torres et al., 2014), and supports the strong control of physical erosion in the weathering of carbonates via oxidative weathering of sulphides. Our chamber-based method provides a new way to quantify this process in the field, and assess the spatial and temporal variability in CO₂ production by this weathering process.

4 Conclusions

Here, we present a reliable, innovative and relatively inexpensive way to measure the flux of CO₂ produced during the oxidative
30 weathering of sedimentary rocks. The ability to trap the CO₂ using active or passive zeolite molecular sieves is essential, since



its carbon isotopic composition (^{12}C , ^{13}C , ^{14}C) is mandatory to assess for atmospheric CO_2 inputs, before partitioning the CO_2 flux between that from oxidation of rock-derived organic carbon and carbonate dissolution by sulphuric acid. The passive method to trap the CO_2 , i.e., leaving zeolite molecular sieve connected to a chamber for days to months, is useful to provide a time integrative sample of CO_2 produced during weathering. This paper is a proof of concept of the oxidative weathering of rocks: i) rock-derived organic carbon is oxidized and CO_2 is released directly to the atmosphere and its flux can be large enough to be directly measurable; ii) the oxidation of sulphides contained in the rocks produces sulphuric acid and dissolves carbonates. In the Laval catchment this phenomenon releases CO_2 directly to the atmosphere rather than dissolved inorganic carbon, and its flux can be locally large.

Data availability

10 Raw data and flux resulting from exponential fitting of data are available in the supplementary material.

Author contribution

RGH conceived the research and designed the study with GS and MHG. GS, RGH and SK carried out chamber installation. GS carried out flux measurements and sample collection with on-field assistance of RGH, MD and MO. GS, RGH, MHG and TC analysed the data. GS, RGH and MHG interpreted the data. GS wrote the manuscript with inputs from RGH and MHG. All co-authors commented on the manuscript.

Acknowledgements

This research was funded by a European Research Council Starting Grant to Robert G. Hilton (ROC- CO_2 project, grant 678779) and by the Natural Environment Research Council (NERC) Radiocarbon Facility (East Kilbride). We thank staff at NERC RCF and SUERC. We thank Jérôme Gaillardet and Caroline Le Bouteiller for collaborative access to the infrastructure at the Draix Bléone Observatory, (IRSTEA).

References

- Bardgett, R. D., Richter, A., Bol, R., Garnett, M. H., Bäuml, R., Xu, X., Lopez-Capel, E., Manning, D. A. C., Hobbs, P. J., Hartley, I. R. and Wanek, W.: Heterotrophic microbial communities use ancient carbon following glacial retreat, *Biol. Lett.*, 3(5), 487–490, doi:10.1098/rsbl.2007.0242, 2007.
- 25 Berner, E. K. and Berner, R. A.: *Global environment: Water, air, and geochemical cycles.*, 2012.
- Berner, R. A. and Canfield, D. E.: A new model for atmospheric oxygen over Phanerozoic time, *Am. J. Sci.*, 289(4), 333–361, doi:10.2475/ajs.289.4.333, 1989.



- Billett, M. F., Garnett, M. H. and Hardie, S. M. L.: A Direct Method to Measure $^{14}\text{CO}_2$ Lost by Evasion from Surface Waters, *Radiocarbon*, 48(1), 61–68, doi:10.1017/S0033822200035396, 2006.
- Blair, N. E., Leithold, E. L., Ford, S. T., Peeler, K. A., Holmes, J. C. and Perkey, D. W.: The persistence of memory: the fate of ancient sedimentary organic carbon in a modern sedimentary system, *Geochim. Cosmochim. Acta*, 67(1), 63–73, doi:10.1016/S0016-7037(02)01043-8, 2003.
- 5 Borges, A. V., Delille, B., Schiettecatte, L.-S., Gazeau, F., Abril, G. and Frankignoulle, M.: Gas transfer velocities of CO_2 in three European estuaries (Randers Fjord, Scheldt, and Thames), *Limnol. Oceanogr.*, 49(5), 1630–1641, doi:10.4319/lo.2004.49.5.1630, 2004.
- Bouchez, J., Beysac, O., Galy, V., Gaillardet, J., France-Lanord, C., Maurice, L. and Moreira-Turcq, P.: Oxidation of petrogenic organic carbon in the Amazon floodplain as a source of atmospheric CO_2 , *Geology*, 38(3), 255–258, doi:10.1130/G30608.1, 2010.
- 10 Calmels, D., Gaillardet, J., Brenot, A. and France-Lanord, C.: Sustained sulfide oxidation by physical erosion processes in the Mackenzie River basin: Climatic perspectives, *Geology*, 35(11), 1003–1006, doi:10.1130/G24132A.1, 2007.
- Calmels, D., Galy, A., Hovius, N., Bickle, M., West, A. J., Chen, M.-C. and Chapman, H.: Contribution of deep groundwater to the weathering budget in a rapidly eroding mountain belt, Taiwan, *Earth Planet. Sci. Lett.*, 303(1–2), 48–58, doi:10.1016/j.epsl.2010.12.032, 2011.
- 15 Copard, Y., Amiotte-Suchet, P. and Di-Giovanni, C.: Storage and release of fossil organic carbon related to weathering of sedimentary rocks, *Earth Planet. Sci. Lett.*, 258(1–2), 345–357, doi:10.1016/j.epsl.2007.03.048, 2007.
- Cras, A., Marc, V. and Travi, Y.: Hydrological behaviour of sub-Mediterranean alpine headwater streams in a badlands environment, *J. Hydrol.*, 339(3–4), 130–144, doi:10.1016/j.jhydrol.2007.03.004, 2007.
- 20 Dalai, T. K., Singh, S. K., Trivedi, J. R. and Krishnaswami, S.: Dissolved rhenium in the Yamuna River System and the Ganga in the Himalaya: Role of black shale weathering on the budgets of Re, Os, and U in rivers and CO_2 in the atmosphere, *Geochim. Cosmochim. Acta*, 66(1), 29–43, doi:10.1016/S0016-7037(01)00747-5, 2002.
- Das, A., Chung, C.-H. and You, C.-F.: Disproportionately high rates of sulfide oxidation from mountainous river basins of Taiwan orogeny: Sulfur isotope evidence, *Geophys. Res. Lett.*, 39(12), doi:10.1029/2012GL051549, 2012.
- 25 Davidson, G. R.: The stable isotopic composition and measurement of carbon in soil CO_2 , *Geochim. Cosmochim. Acta*, 59(12), 2485–2489, doi:10.1016/0016-7037(95)00143-3, 1995.
- Galy, A. and France-Lanord, C.: Weathering processes in the Ganges–Brahmaputra basin and the riverine alkalinity budget, *Chem. Geol.*, 159(1–4), 31–60, doi:10.1016/S0009-2541(99)00033-9, 1999.
- 30 Galy, V., Beysac, O., France-Lanord, C. and Eglinton, T.: Recycling of Graphite During Himalayan Erosion: A Geological Stabilization of Carbon in the Crust, *Science*, 322(5903), 943–945, doi:10.1126/science.1161408, 2008.
- Garnett, M. H. and Hardie, S. M. L.: Isotope (^{14}C and ^{13}C) analysis of deep peat CO_2 using a passive sampling technique, *Soil Biol. Biochem.*, 41(12), 2477–2483, doi:10.1016/j.soilbio.2009.09.004, 2009.



- Garnett, M. H. and Murray, C.: Processing of CO₂ Samples Collected Using Zeolite Molecular Sieve for ¹⁴C Analysis at the NERC Radiocarbon Facility (East Kilbride, UK), *Radiocarbon*, 55(2), 410–415, doi:10.1017/S0033822200057532, 2013.
- Garnett, M. H., Hartley, I. P., Hopkins, D. W., Sommerkorn, M. and Wookey, P. A.: A passive sampling method for radiocarbon analysis of soil respiration using molecular sieve, *Soil Biol. Biochem.*, 41(7), 1450–1456, doi:10.1016/j.soilbio.2009.03.024, 2009.
- 5 Graz, Y., Di-Giovanni, C., Copard, Y., Mathys, N., Cras, A. and Marc, V.: Annual fossil organic carbon delivery due to mechanical and chemical weathering of marly badlands areas, *Earth Surf. Process. Landforms*, 37(12), 1263–1271, doi:10.1002/esp.3232, 2012.
- Hahn, V., Högberg, P. and Buchmann, N.: ¹⁴C - A tool for separation of autotrophic and heterotrophic soil respiration, *Glob. Chang. Biol.*, 12(6), 972–982, doi:10.1111/j.1365-2486.2006.001143.x, 2006.
- 10 Hardie, S. L. M. L., Garnett, M. H. H., Fallick, a. E. E., Rowland, a. P. P. and Ostle, N. J. J.: Carbon dioxide capture using a zeolite molecular sieve sampling system for isotopic studies (¹³C and ¹⁴C) of respiration, *Radiocarbon*, 47(3), 441–451, doi:10.2458/azu_js_rc.v.2838, 2005.
- Hilton, R. G., Galy, A., Hovius, N., Horng, M. J. and Chen, H.: Efficient transport of fossil organic carbon to the ocean by steep mountain rivers: An orogenic carbon sequestration mechanism, *Geology*, 39(1), 71–74, doi:10.1130/G31352.1, 2011.
- 15 Hilton, R. G., Gaillardet, J., Calmels, D. and Birck, J. L.: Geological respiration of a mountain belt revealed by the trace element rhenium, *Earth Planet. Sci. Lett.*, 403, 27–36, doi:10.1016/j.epsl.2014.06.021, 2014.
- Horan, K., Hilton, R. G., Selby, D., Ottley, C. J., Gröcke, D. R., Hicks, M. and Burton, K. W.: Mountain glaciation drives rapid oxidation of rock-bound organic carbon, *Sci. Adv.*, 3(10), e1701107, doi:10.1126/sciadv.1701107, 2017.
- 20 Jaffe, L. A., Peucker-Ehrenbrink, B. and Petsch, S. T.: Mobility of rhenium, platinum group elements and organic carbon during black shale weathering, *Earth Planet. Sci. Lett.*, 198(3–4), 339–353, doi:10.1016/S0012-821X(02)00526-5, 2002.
- Keller, C. K. and Bacon, D. H.: Soil respiration and georespiration distinguished by transport analyses of vadose CO₂, ¹³CO₂, and ¹⁴CO₂, *Global Biogeochem. Cycles*, 12(2), 361–372, doi:10.1029/98GB00742, 1998.
- Kutzbach, L., Schneider, J., Sachs, T., Giebels, M., Nykänen, H., Shurpali, N. J., Martikainen, P. J., Alm, J. and Wilmking, M.: CO₂ flux determination by closed-chamber methods can be seriously biased by inappropriate application of linear regression, *Biogeosciences Discuss.*, 4(4), 2279–2328, doi:10.5194/bgd-4-2279-2007, 2007.
- 25 Li, S. L., Calmels, D., Han, G., Gaillardet, J. and Liu, C. Q.: Sulfuric acid as an agent of carbonate weathering constrained by δ¹³C DIC: Examples from Southwest China, *Earth Planet. Sci. Lett.*, 270(3–4), 189–199, doi:10.1016/j.epsl.2008.02.039, 2008.
- 30 Mathys, N., Brochot, S., Meunier, M. and Richard, D.: Erosion quantification in the small marly experimental catchments of Draix (Alpes de Haute Provence, France). Calibration of the ETC rainfall–runoff–erosion model, *CATENA*, 50(2–4), 527–548, doi:10.1016/S0341-8162(02)00122-4, 2003.
- Mook, W. G. and van der Plicht, J.: Reporting ¹⁴C Activities and Concentrations, *Radiocarbon*, 41(3), 227–239, doi:10.1017/S0033822200057106, 1999.



- Petsch, S. T.: Weathering of Organic Carbon, in *Treatise on Geochemistry*, vol. 12, pp. 217–238, Elsevier., 2014.
- Petsch, S. T., Berner, R. A. and Eglinton, T. I.: A field study of the chemical weathering of ancient sedimentary organic matter, in *Organic Geochemistry*, vol. 31, pp. 475–487., 2000.
- Petsch, S. T., Eglinton, T. I. and Edwards, K. J.: ¹⁴C-Dead Living Biomass: Evidence for Microbial Assimilation of Ancient
5 Organic Carbon During Shale Weathering, *Science*, 292(5519), 1127–1131, doi:10.1126/science.1058332, 2001.
- Pirk, N., Mastepanov, M., Parmentier, F.-J. W., Lund, M., Crill, P. and Christensen, T. R.: Calculations of automatic chamber
flux measurements of methane and carbon dioxide using short time series of concentrations, *Biogeosciences*, 13(4), 903–
912, doi:10.5194/bg-13-903-2016, 2016.
- Reimer, P. J., Brown, T. A. and Reimer, R. W.: Discussion: reporting and calibration of post-bomb ¹⁴C data., *Radiocarbon*,
10 46(1), 1299–1304, doi:10.2458/azu_js_rc.46.4183, 2004.
- Stuiver, M. and Polach, H. A.: Discussion Reporting of ¹⁴C Data, *Radiocarbon*, 19(3), 355–363,
doi:10.1017/S0033822200003672, 1977.
- Sundquist, E. T. and Visser, K.: Geologic history of the carbon cycle, in *Biogeochemistry*, pp. 425–472., 2005.
- Torres, M. A., West, A. J. and Li, G.: Sulphide oxidation and carbonate dissolution as a source of CO₂ over geological
15 timescales, *Nature*, 507(7492), 346–349, doi:10.1038/nature13030, 2014.

20

25

30



Tables

Table 1. Dimensions of a typical chamber^{a, b}

Inner diameter	Depth	PVC tubing	Depth of insertion of PVC tubing	Depth of insertion of rubber stopper	Chamber volume	Area of exchange with surrounding rock
cm	cm	cm	cm	cm	cm ³	cm ²
2.9 (2.8 - 3.0)	41 (40.5 - 41.5)	4 (3.5 - 4.5)	1.5 (1 - 2)	1 (0.75 - 1.25)	281 (252 - 312)	366 (345 - 389)

^aChamber H6 drilled on 13/12/2016 in the catchment of the Laval stream (Draix, France; N44.14061°, E06.36289°)

^bGiven as ranges: median (min - max)

5

Table 2. Isotopic composition of the CO₂ sampled with the zeolite molecular sieves

Sample label	Publication number	Method	Mass of carbon sampled (mg)	δ ¹³ C (‰VPDB)	Fraction modern
DRA16-H6-1512-P	SUERC-73091	Passive ^a	11.4	-9.4	0.0495 ± 0.0047
DRA17-H6-2803-A	SUERC-73096	Active	2.1	-7.4	0.0597 ± 0.0047
DRA17-H6-3003-A	SUERC-73094	Active	2.1	-6.1	0.0562 ± 0.0047
DRA17-ATM-2703	SUERC-73095	Active	3.8	-9.6	1.0065 ± 0.0044

^a sampled passively for 100.84 days

10

Table 3. Geochemical composition of the rock sampled during the drilling of chamber H6^a

	Content (weight %)	Publication number	δ ¹³ C (‰VPDB)	Fraction modern
Total Inorganic Carbon	6.52±0.6 (n=3)	SUERC-74506	0.3 ± 0.1	0.0032 ± 0.0006
Total Organic Carbon	0.11±0.7 (n=3)	UCIAMS-192874	-30.8 ± 0.1	0.0125 ± 0.0039

^ain house label of this sample was DRA16-78

**Table 4. Isotope-mass balance results**

Sample label	Publication number	Method	Sources	Proportion (%)	Proportion corrected for atmospheric contribution (%)	Partitioned flux (gC.m ⁻² .yr ⁻¹)
DRA16-H6-1512-P	SUERC-73091	Passive ^a	Atmosphere	4.9 ± 0.5	–	–
			Carbonates	76.7 ± 1.5	80.7 ± 1.6	–
			Rock Organic Carbon	18.4 ± 1.5	19.3 ± 1.6	–
DRA17-H6-2803-A	SUERC-73096	Active	Atmosphere	5.9 ± 0.5	–	–
			Carbonates	71.2 ± 0.5	75.7 ± 0.4	206 ± 6 ^b
			Rock Organic Carbon	22.9 ± 0.4	24.3 ± 0.4	66 ± 2 ^b
DRA17-H6-3003-A	SUERC-73094	Active	Atmosphere	5.6 ± 0.5	–	–
			Carbonates	75.6 ± 0.5	80.1 ± 0.4	–
			Rock Organic Carbon	18.8 ± 0.4	19.9 ± 0.4	–

^a before solving isotope-mass balance, the $\delta^{13}\text{C}$ of the passive sample was corrected for a fractionation factor of 3.50 ± 0.45 (Garnett et al., 2009)

^b from a measured bulk CO₂ flux of 272 ± 8 gC.m⁻².yr⁻¹

5

10



Figures

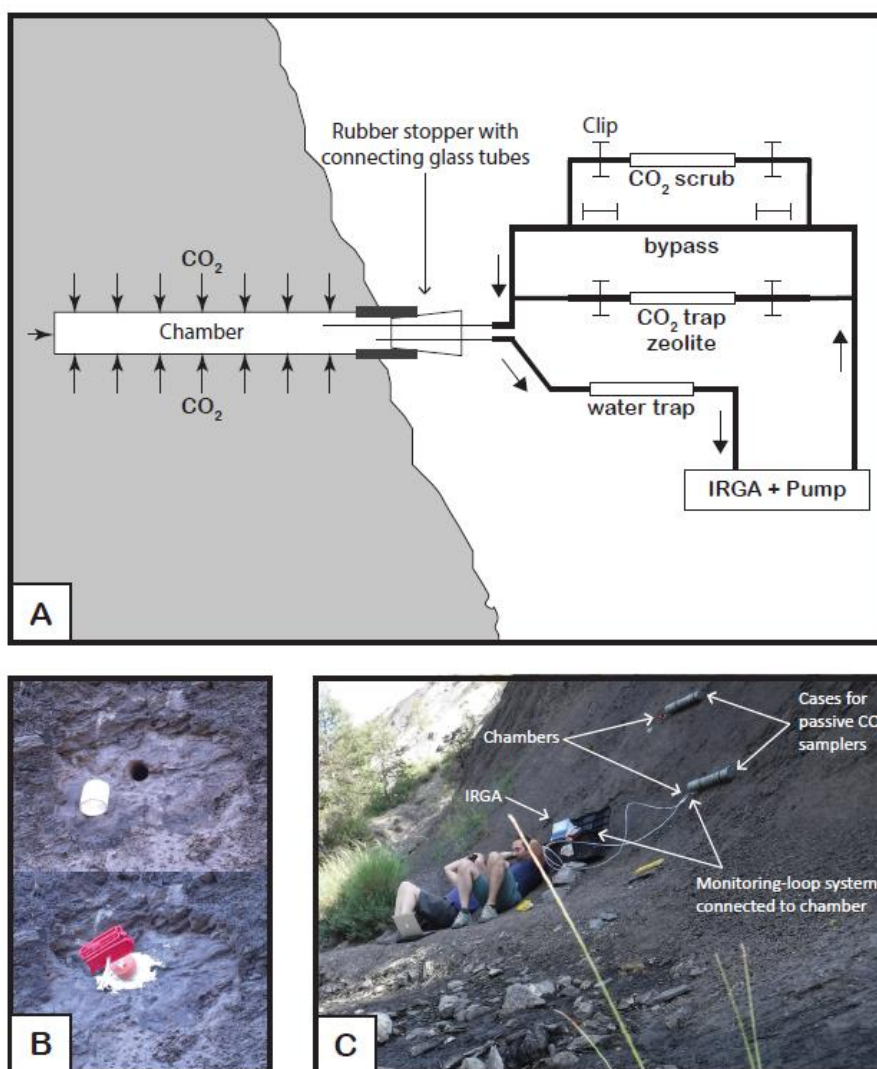


Figure 1: A: Schematic diagram of the closed-loop monitoring-sampling system connected to the natural weathering chamber. Gas flow pathways are controlled by opening and closing the clips. Clips removed from the bypass allow pCO₂ in the chamber to be monitored (IRGA stands for Infra-Red Gas Analyzer), thus measuring CO₂ flux and ensuring that enough CO₂ accumulated in the chamber for ¹⁴C analysis. To remove CO₂ from the line before connecting to the chamber, clips are moved from the CO₂ scrub (soda lime). When connected to the chamber, the CO₂ scrub can be used to lower the CO₂ concentration before flux measurement. To collect CO₂ in the chamber for isotope analyses, clips are removed from the zeolite molecular sieve cartridge. B: Pictures showing the chamber design. Top picture is chamber (H6), diameter 2.9cm, drilled in the rock on a cleared surface, with white PVC tubing inserted at the outlet. Bottom picture shows the rubber stopper fitted in the PVC tubing. Two glass tubes go through the rubber stopper and are fitted with Tygon tubing, sealed with the red clips, and the exterior of the chamber is sealed with outdoor sealant. C: View of the field site showing two chambers (top chamber is H6 and lower chamber is H4). The lower chamber is connected to the closed-loop system and is being monitored for flux measurement. The two large grey PVC tubes attached to the rock on the right of the chambers are cases in which zeolite molecular sieves are installed and left for months when connected to the chamber for passive CO₂ trapping.

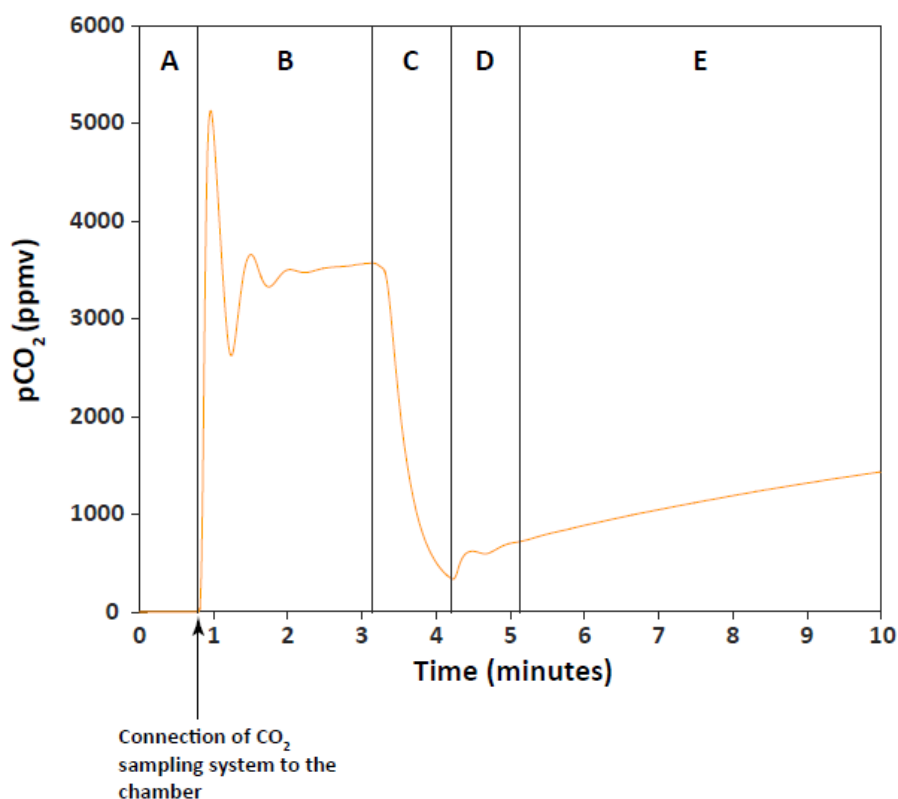


Figure 2: An example of the monitoring of the CO₂ accumulating in a chamber. The orange curve is the partial pressure of CO₂ (pCO₂, in parts per million volume) through time in chamber H6 on 27/03/2017. A: The CO₂ sampling-monitoring system is not connected to the chamber. Atmospheric CO₂ has been removed from the system (pCO₂ = 0 ppm) using the CO₂ scrub cartridge. B: The closed-loop monitoring system has been connected to the chamber. pCO₂ increases to reach a maximum value of ~5100 ppm, then drops and equilibrates to ~3500ppm. This pattern reflects the increase in the total volume (by the volume of the CO₂ sampling-monitoring system) which decreases pCO₂ and requires some time for the pCO₂ to equilibrate. We determined that when connected to the chamber, the maximum value of pCO₂ read is 0.94 the actual pCO₂ in the chamber. C: The CO₂ in the chamber is lowered (scrubbed with the CO₂ scrub, or trapped with the zeolite molecular sieve) to near atmospheric pCO₂. D: residual CO₂ that in the chamber homogenized with the rest of the total volume “artificially” increasing pCO₂ quickly. E: pCO₂ in chamber is monitored, reflecting the flux of CO₂ from the rock surface to the chamber.

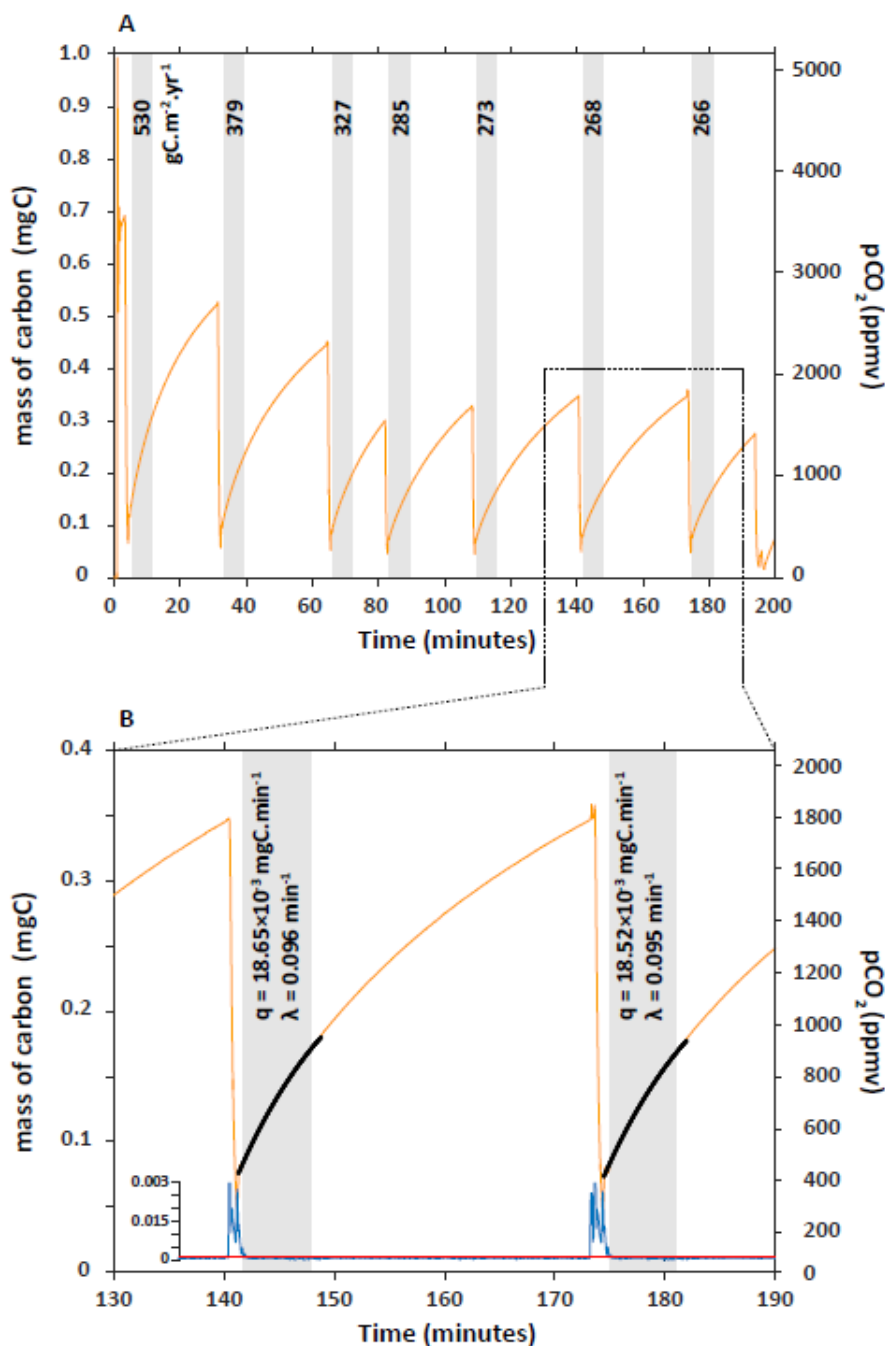


Figure 3: A: Series of carbon flux measurements for chamber H6 on 27/03/2017. CO_2 concentration (pCO_2) was converted into mass of carbon (mgC) following Eq. (4) and Eq. (5). Flux of CO_2 – the numbers associated to shaded boxes – are given in $\text{gC.m}^{-2}.\text{yr}^{-1}$. B: Close-up of how fluxes were calculated from the rate of carbon accumulation (parameter q) by fitting the exponential model described in Eq. (7) and (8) for 6 minutes (shaded box) after a 10-sec moving window variability in the rate of mass carbon change (blue curve) was below a threshold of $10^{-4} \text{ mgC.min}^{-1}$ (red line).

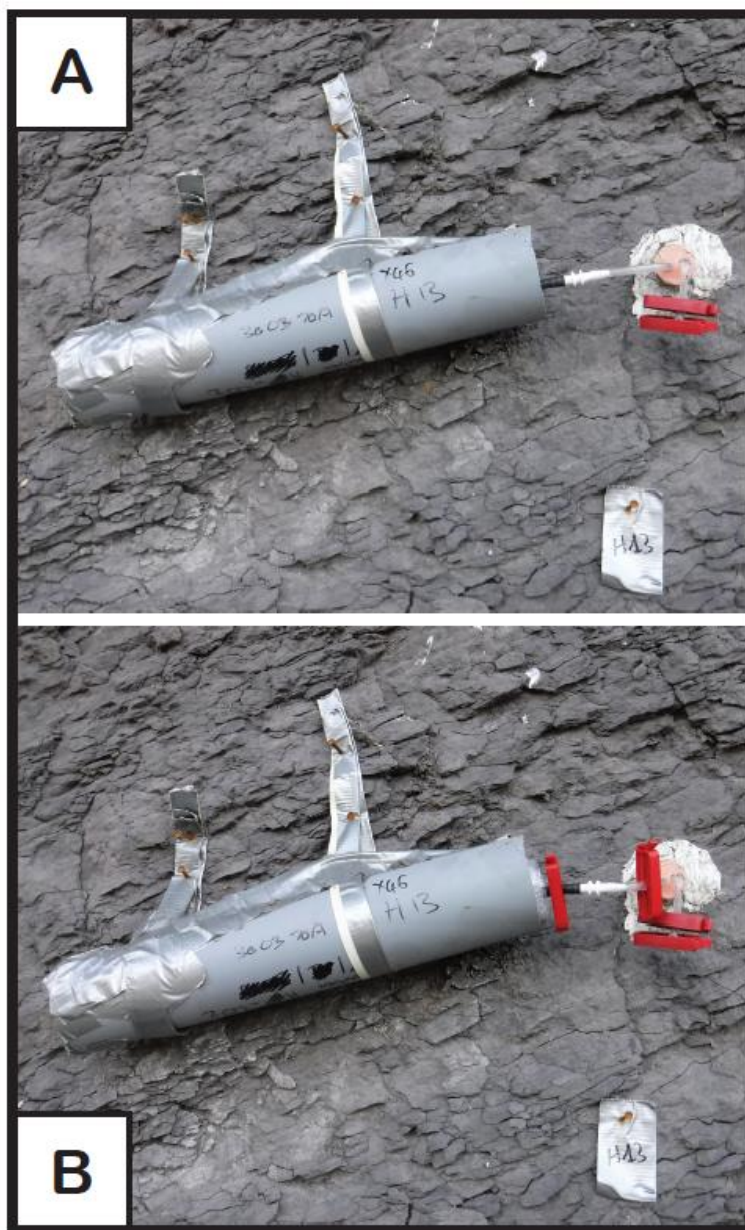


Figure 4: A: Zeolite molecular sieve connected to a chamber for passive CO₂ trapping. The zeolite molecular sieve is encased in the grey PVC tubing and connected for months to the chamber using a white connector. B: Zeolite molecular sieve ready to be disconnected from chamber. The red clips are positioned so that they seal both the zeolite molecular sieve and the chamber.